Published in final edited form as:
*Angew Chem Int Ed Engl*. 2017 February 20; 56(9): 2508–2512. doi:10.1002/anie.201610441.

# Proton-detected solid-state NMR spectroscopy of a zinc diffusion facilitator protein in native nanodiscs

**Dr. Beate Bersch**[a],*, **Jonas M. Dörr**[b], **Audrey Hessel**[a], **J. Antoinette Killian**[b], and **Dr. Paul Schanda**[a],*

[a]CEA, CNRS, Univ. Grenoble Alpes, Institut de Biologie Structurale 71, avenue des martyrs, F-38044 Grenoble, France [b]Membrane Biochemistry and Biophysics Bijvoet Center for Biomolecular Research, Utrecht University, Padualaan 8, 3584 CH Utrecht, Netherlands

## Abstract

The structure, dynamics and function of membrane proteins are intimately linked to the properties of the membrane environment in which the proteins are embedded. For structural and biophysical characterization, membrane proteins generally need to be extracted from the membrane, and reconstituted in a suitable membrane-mimicking environment. Ensuring functional and structural integrity in these environments is often a major concern. The styrene/maleic acid co-polymer has recently been shown to be able to extract lipid/membrane protein patches directly from native membranes, forming nanosize discoidal proteolipid particles, also referred to as native nanodiscs. Here we show, for the first time, that high-resolution solid-state NMR spectra can be obtained from an integral membrane protein in native nanodiscs, as exemplified with the 2 x 34 kDa-large bacterial cation diffusion facilitator CzcD from *Cupriavidus metallidurans* CH34.

### Keywords

membrane protein; nanodiscs; styrene maleic acid; NMR spectroscopy; solid-state NMR

Integral membrane proteins play essential roles in numerous cellular processes. The properties of the surrounding lipid environment are crucial to their structure, dynamics and function. However, structural and biophysical characterizations by most biophysical techniques generally require extraction and purification from the native membrane. Major concerns when working with detergent-solubilized membrane proteins are related to the fact that functionally and structurally important lipids are often stripped away, and that the properties of the detergent micelle differ significantly from the planar lipid bilayer environment. An increasing number of cases of distortions of membrane protein structures in detergents have been reported.[1,2] These known problems with detergents have triggered the development of alternative non-micellar systems, such as amphiphilic polymers (amphipols), bicelles, or nanolipoprotein particles, i.e. a lipid patch surrounded by a membrane-scaffold protein.[3–5] A particularly interesting recent approach is the use of the

beate.bersch@ibs.fr, paul.schanda@ibs.fr.


Europe PMC Funders Author Manuscripts

styrene/maleic acid co-polymer (SMA), which is able to self-insert into the lipid bilayer, and to extract membrane proteins directly from the membrane, forming nanosize disc-shaped particles.[5–7] SMA has been successfully used to solubilize membrane proteins from reconstituted proteoliposomes[8,9], and also from native cellular membranes, forming so-called native nanodiscs.[7,10–14] The stability and activity of proteins in SMA-bounded nanodiscs have been shown to be significantly higher than in detergent micelles in several instances, and some cases were reported where the stability was even higher than in the native membrane[15]. These nanodiscs have been used in functional tests, ligand binding studies, electron-microscopy, EPR and other spectroscopic characterizations (reviewed in ref. [16]). Here we show that membrane proteins in native nanodiscs are amenable to atomic-resolution studies using magic-angle spinning solid-state NMR (MAS ssNMR) spectroscopy. We exemplify this with the integral membrane protein CzcD from *Cupriavidus metallidurans* CH34, a zinc diffusion facilitator of 34 kDa molecular weight. In *C. metallidurans* CH34, CzcD is part of a cobalt-zinc-cadmium resistance system (Czc).[17] Based on homology to proteins of known structure, CzcD is assumed to form homodimers. Currently, structural information on full-length proteins of this family is available from two bacterial cation-diffusion-facilitator (CDF) proteins, one in an outward-facing state[18] (*Escherichia coli* Yiip, see homology model in Figure 1a), the other in an inward-facing state[19] (*Shewanella oneidensis* YiiP). These structures may represent the two states of an alternate access mechanism. However, as structural information has been obtained from protein reconstituted in detergent micelles[18] or tubular crystals[19], characterization of the conformational change in response to $Zn^{2+}$ ions in a more physiological membrane environment would be of great importance for the decryption of its transport mechanism. Direct solubilization in the form of native nanodiscs combined with high-resolution solid-state NMR spectroscopy therefore would be a promising approach towards revealing the details of the way CDF proteins exert cation transport across the membrane.

When expressed in *E. coli*, we found that CzcD was directly inserted into the cytoplasmic membrane. After cell lysis, the membrane fraction was isolated and incubated with SMA polymers (see Figures S1-S3 and detailed experimental methods in the Supporting Information). SMA-solubilized CzcD was purified using a Strep-Tactin affinity chromatography, demonstrating that this type of affinity purification can be successfully used for proteins solubilized with SMA. The Strep tag was preferred over His-tag because it does not interfere with metal binding to the protein. Figure 1b shows a size exclusion chromatography (SEC) profile of a nanodisc-embedded CzcD sample. The chromatogram shows two major peaks eluting at 48 and 67 mL with a smaller shoulder at 58 mL. Negative-staining electron microscopy images of these three fractions are shown in Figure 1c. The first protein-containing fraction contains relatively large, liposome-like particles and may correspond to incompletely solubilized membrane fragments. Electron micrographs from fraction 2 show a relatively non-homogenous population of significantly smaller particles of approximately 15-20 nm diameter. Finally, a homogenous population of nanodiscs with a size of 10-15 nm is obtained in the third fraction. Dynamic light scattering experiments of an independent batch with higher homogeneity confirm these findings (Fig. S4). Using a phosphorous assay, we determined 32-35 lipids per protein dimer, which corresponds to

about one layer of lipid around the protein (see details in the Supporting Information). Similar lipid-protein ratios were found in previous reports[8,12].

To explore the possibility to obtain atomic-resolution NMR information of these native-nanodisc samples of CzcD we sedimented nanodisc-containing fractions (i.e. peaks 2 and 3 of the chromatogram shown in Figure 1b, or equivalent peaks from other purifications) into a 1.3 mm solid-state NMR sample rotor by ultracentrifugation (about 3 μL sample volume). We used three different isotope labeling schemes in this study, (i) uniform $^{13}C$,$^{15}N$ labeling, (ii) uniform $^{2}H$,$^{13}C$,$^{15}N$ labeling and (iii) deuteration and selective labeling of Ile-δ1 sites with $CH_3$ groups.

Figure 2 shows one-dimensional $^{13}C$- and $^{15}N$-detected spectra of CzcD in native nanodiscs, providing a first impression of the sample and of its composition. The direct-excitation $^{13}C$ spectrum reveals as most prominent features a number of sharp signals in the aliphatic region (10-60 ppm), in the region of 120-130 ppm, in which olefinic and aromatic carbons resonate, which likely stem from lipids. Furthermore, resonances in the carbonyl (170-180 ppm), the aliphatic (10-60 ppm) and the aromatic (120-140 ppm) regions can be ascribed to protein signals. By comparison with the signal intensity of the carbonyl (i.e. protein) signals, signals around 120 ppm cannot arise exclusively from the protein but also include contributions from olefinic lipid carbons. In $^{13}C$ spectra obtained with $^{1}H$-$^{13}C$ cross-polarization (CP, Fig. 2c), the lipid signals also dominate. The $^{13}C$ CP spectrum obtained with the deuterated sample (Fig. 2d) shows strongly reduced signal intensity, compared to the direct-excitation $^{13}C$ spectrum (Fig. 2b) and to the CP spectrum of the protonated sample (Fig. 2a). This is expected in such $^{1}H$-$^{13}C$ CP spectra, due to the absence of protons; the observed signals, primarily of carbonyl and $C^{\alpha}$ sites, are due to cross-polarization from the re-protonated amide $H^{N}$ sites. Finally, the $^{15}N$ spectrum (Fig. 2e,f) reveals an intense backbone amide signal, as well as signals corresponding to His, Arg and Lys side chains. We also collected INEPT-based correlation experiments, which detect only highly flexible C-H sites; such a spectrum shows only lipid signal, suggesting that CzcD is devoid of extended stretches of highly flexible residues (see Fig. S6 in the Supporting Information).

We next investigated the dynamical properties of CzcD in native nanodiscs. At this stage we were interested in overall properties, and in particular the question whether nanodisc-embedded CzcD undergoes fast axial rotation inside the nanodisc (which itself is immobilized because of the sedimentation brought about by MAS). Such axial rotation has been shown for several membrane proteins in liposomes[20,21]. The presence of fast axial rotation is expected to strongly reduce dipolar order parameters. (Strictly speaking the dipolar coupling of $^{1}H$-$^{15}N$ bonds that are parallel to the rotation axis is not reduced, but often an overall reduction by approximately a factor 2 is seen even for proteins with no extramembrane domains, see e.g. ref. [21,22]. In CzcD with its cytoplasmic domain the N-H bonds are distributed almost uniformly, such that overall rotation would result in significant reduction of the dipolar coupling.) If such overall rotation of the molecules occurs on a nanosecond-to-microsecond time scale, $^{15}N$ $R_{1\rho}$ spin relaxation rate constants are expected to be enhanced. Finally, $R_1$ relaxation rate constants are sensitive to motions if they occur on shorter (ps-ns) time scales. We thus recorded bulk measurements of these three dynamic parameters, integrated over all amide signals, using robust approaches based on deuterated

protein and high MAS frequency (Figure 2h,g and Figure S7). The dynamics observables reveal that CzcD does not undergo fast axial rotation in nanodiscs: H-N dipolar order parameter are fairly high (S~0.8, Figure 2h), reflecting presumably mostly local motion in an otherwise rigid molecular frame. These order parameters are slightly lower than those found in crystalline proteins that undergo only local motions (where S~0.85-0.9). Interestingly, this finding also suggests that the cytoplasmic domain does not undergo large-scale motion with respect to the transmembrane domain. Likewise, both $R_1$ and $R_{1\rho}$ rate constants are similar to values found in microcrystalline proteins[23] devoid of overall motion. These parameters do not show significant temperature dependence over the probed temperature range (270-298 K, Figure 2h). Taken together, these observations point to an absence of overall axial rotation of CzcD within nanodiscs. This finding appears reasonable, considering the large size of the CzcD dimer and the relatively low lipid-protein ratio (see above). The apparent absence of large-scale ns-μs motions (low $R_{1\rho}$ rate constants) also leads us to predict that transverse relaxation time constants, $T_2$' are also long. As line widths depend on these coherence life times, this is an important parameter. Indeed, we find relatively long $T_2$' life times of the order of 25-30 ms for $^{15}N$ and $^{13}C'$, and about 4 ms for $^{1}H$ (see Table S2). Although best-behaving crystalline proteins have typically slower coherence decays (by ~a factor of 2-3; see ref. [24] and Table S2), our data suggest that it should be possible to obtain high-resolution spectra of nanodisc-embedded CzcD.

To evaluate the potential of obtaining such atomic-resolution information, we then performed three-dimensional $^{1}H$-$^{15}N$-$^{13}C$ correlation experiments. With 2x34 kDa molecular weight, CzcD is a very large protein for ssNMR applications, and the corresponding spectral complexity and sensitivity penalty make 3D ssNMR spectroscopy challenging. To date, no protein of this size, including non-membrane proteins, has been assigned by ssNMR, to our knowledge, highlighting this challenge. As an additional complication, the sample amount is often limited, particularly for membrane proteins. For the case of CzcD, we obtained about 1-4 mg of protein per liter of culture; traditional ssNMR approaches with $^{13}C$-detection typically require 10-20 mg of protein. With these requirements of sensitivity and resolution in mind, we turned to deuteration and selective re-protonation of amide or methyl sites, combined with fast-MAS and proton-detected experiments, because of the high detection sensitivity and resolution. Indeed, we were able to obtain three-dimensional H-N-C spectra at fast (55 kHz) MAS within 3.5-5 days (see Supporting Information Methods). Figure 3a shows a hCANH experiment, correlating the amide proton and nitrogen frequencies to the intra-residue $C^{\alpha}$, and panel b shows a hCONH experiment[25], connecting the amide moiety to the C' of the preceding residue. Projections of these 3D spectra, and further 2D planes thereof are shown in Fig. S9. Typical amide $^{1}H$ line widths are of the order of 50-70 Hz, narrower than line widths obtained on 2D-crystals of β-barrel membrane proteins,[26] or on a sample of liposome-embedded proteorhodopsin (a protein that yields highly resolved $^{13}C$-detected spectra)[27]. $^{1}H$ line widths of methyls, obtained with $CH_3$-labelling[28] of Ile-δ1 sites are as low as ~30-40 Hz (Figure 3c). Notwithstanding these fairly favorable line widths, the large number of residues (more than 300) leads to severe resonance overlap, hampering assignment, and making it difficult to evaluate the completeness of these spectra.

In order to assist the assignment, we prepared samples of the isolated cytoplasmic (soluble) C-terminal domain ($CzcD_{209-316}$) and obtained solution-state NMR assignments with and without zinc (see Fig. S7). Solution-state diffusion-ordered spectroscopy showed that the in the presence of two equivalent zinc the protein dimerizes. With these assignments at hand, we identified 13 spin systems, in 3 stretches of the cytoplasmic domain, which closely match in the four frequencies we observe ($^{1}H$, $^{15}N$, $^{13}C^{\alpha}$ and $^{13}C'$) to resonance peaks in the full-length ssNMR spectrum (6 of which are shown in Figure 3a,b), allowing to transfer assignments. Interestingly, the closest similarity is found to the spectra of the $Zn^{2+}$ form (Table S3). This finding suggests that full-length CzcD in nanodiscs is in a $Zn^{2+}$-bound and presumably dimeric form, as expected from the available crystal structures. We note that for a >300-residue large membrane protein assignment remains challenging in terms of resolution and sensitivity, and further 3D experiments, in addition to the two experiments shown here will be required for unambiguous assignment.

Figure 3c compares the methyl HC correlation spectra of soluble and full-length proteins. The relatively large number of expected cross-peaks (20 in the TM part and 4 in the cytoplasmic domain), and the fact that methyls in TM parts tend to experience very similar environments and thus similar chemical shifts, limits resolution. Nonetheless, the assigned Ile cross-peaks from the soluble domain can be identified in the full-length CzcD, and they appear distinct from the TM Ile peaks (Figure 3c). Interestingly, these methyl resonances show some chemical-shift differences to the isolated cytoplasmic domain, suggesting that the presence of the TM domain and the lipid bilayer alters the packing of the dimerizing cytoplasmic domains.

To summarize, we have shown here that membrane proteins directly extracted from the bacterial membrane using SMA polymers yield state-of-the-art MAS ssNMR spectra, opening the way for ssNMR studies of these challenging proteins. The present example of a 2x34 kDa large cation diffusion facilitator shows that favorable line widths are obtained, enabling high-resolution studies. This approach does not require conventional detergents in any step, which is an advantage over membrane-scaffold-protein based nanodiscs, which have also been used for NMR studies.[29,30] The low amount of copurified lipid may reflect a more limited environment than the native membrane, however this also leads to an enrichment of the protein mass fraction in the ssNMR rotor, leading to increased sensitivity. The lipids that are extracted with the protein have the same isotope labeling as the protein, without any excess cost e.g. for deuterated lipids, used to to enhance sensitivity and resolution.[26] Native nanodiscs may also be an interesting alternative to recently reported NMR approaches performed on native membrane preparations or whole cells.[31,32] These “in-membrane NMR” approaches allow studying over-expressed proteins directly in the membrane, but they suffer from the often-low amount of target protein, and from the presence of other membrane proteins. Native nanodiscs overcome these limitations, as the target protein can be affinity-purified and thus enriched, in a form that is stable on the time scales of NMR experiments. We believe that this approach is versatile: the ability of SMA to extract membrane proteins either from the native membrane or reconstituted liposomes has been demonstrated with different types of membrane proteins (α-helical, β-barrels).[16] Properties important for NMR sensitivity, such as the lipid-protein ratio, are similar in these

other reported cases, suggesting that the favorable ssNMR properties revealed in this study are likely general for other SMA-nanodisc embedded proteins.

## Supplementary Material

Refer to Web version on PubMed Central for supplementary material.

## Acknowledgements

We thank Prof. Sandro Keller, Jessica Klement, Dr. Vilius Kurauskas and Katharina Weinhäupl for insightful discussions. We thank Daphna Fenel and Dr Christine Moriscot for the collection of electron-microscopy data. This work was supported by the European Research Council (ERC-StG 311318-ProtDyn2Function), the CEA, CNRS and Université Grenoble Alpes. JMD and JAK acknowledge financial support via the Seventh Framework Program of the European Union (Marie Curie Initial Training Network "ManiFold", Grant No. 317371). We thank Polyscope for their kind gift of SMA. This work used the platforms of the Grenoble Instruct Center (ISBG; UMS 3518 CNRS-CEA-UJF-EMBL) with support from FRISBI (ANR-10-INSB-05-02) and GRAL (ANR-10-LABX-49-01) within the Grenoble Partnership for Structural Biology (PSB). The electron microscope facility is supported by the Rhône-Alpes Region, the Fondation Recherche Medicale (FRM), the fonds FEDER, and the GIS-Infrastrutures en Biologie Sante et Agronomie (IBISA).

## References

[1]. Zoonens M, Comer J, Masscheleyn S, Pebay-Peyroula E, Chipot C, Miroux B, Dehez F. J Am Chem Soc. 2013; 135:15174–15182. [PubMed: 24021091]

[2]. Zhou H-X, Cross TA. Ann Rev Biophys. 2013; 42:361–392. [PubMed: 23451886]

[3]. Popot JL, Althoff T, Bagnard D, Banères JL, Bazzacco P, Billon-Denis E, Catoire LJ, Champeil P, Charvolin D, Cocco MJ, et al. Ann Rev Biophys. 2011; 40:379–408. [PubMed: 21545287]

[4]. Durr UHN, Gildenberg M, Ramamoorthy A. Chem Rev. 2012; 112:6054–6074. [PubMed: 22920148]

[5]. Nath A, Atkins WM, Sligar SG. Biochemistry. 2007; 46:2059–2069. [PubMed: 17263563]

[6]. Orwick MC, Judge PJ, Procek J, Lindholm L, Graziadei A, Engel A, Gröbner G, Watts A. Angew Chem Int Ed Engl. 2012; 51:4653–4657. [PubMed: 22473824]

[7]. Long AR, O'Brien CC, Malhotra K, Schwall CT, Albert AD, Watts A, Alder NN. BMC Biotechnol. 2013; 13:41. [PubMed: 23663692]

[8]. Knowles TJ, Finka R, Smith C, Lin Y-P, Dafforn T, Overduin M. J Am Chem Soc. 2009; 131:7484–7485. [PubMed: 19449872]

[9]. Sahu ID, McCarrick RM, Troxel KR, Zhang R, Smith HJ, Dunagan MM, Swartz MS, Rajan PV, Kroncke BM, Sanders CR, et al. Biochemistry. 2013; 52:6627–6632. [PubMed: 23984855]

[10]. Gulati S, Jamshad M, Knowles TJ, Morrison KA, Downing R, Cant N, Collins R, Koenderink JB, Ford RC, Overduin M, et al. Biochem J. 2014; 461:269–278. [PubMed: 24758594]

[11]. Paulin S, Jamshad M, Dafforn TR, Garcia-Lara J, Foster SJ, Galley NF, Roper DI, Rosado H, Taylor PW. Nanotechnology. 2014; 25:285101. [PubMed: 24972373]

[12]. Postis V, Rawson S, Mitchell JK, Lee SC, Parslow RA, Dafforn TR, Baldwin SA, Muench SP. Biochim Biophys Acta. 2015; 1848:496–501. [PubMed: 25450810]

[13]. Jamshad M, Charlton J, Lin Y-P, Routledge SJ, Bawa Z, Knowles TJ, Overduin M, Dekker N, Dafforn TR, Bill RM, et al. Biosci Rep. 2015; 35(2):1–10. DOI: 10.1042/BSR20140171

[14]. Dörr JM, Koorengevel MC, Schäfer M, Prokofyev AV, Scheidelaar S, van der Cruijsen EAW, Dafforn TR, Baldus M, Killian JA. P Natl Acad Sci Usa. 2014; 111:18607–18612.

[15]. Swainsbury DJK, Scheidelaar S, van Grondelle R, Killian JA, Jones MR. Angew Chem Int Edit. 2014; 53:11803–11807.

[16]. Dörr JM, Scheidelaar S, Koorengevel MC, Dominguez JJ, Schäfer M, van Walree CA, Killian JA. Eur Biophys J. 2016; 45(1):3–21. DOI: 10.1007/s00249-015-1093-y [PubMed: 26639665]

[17]. Anton A, Grosse C, Reissmann J, Pribyl T, Nies DH. J Bacteriol. 1999; 181:6876–6881. [PubMed: 10559151]

[18]. Lu M, Chai J, Fu D. Nat Struct Mol Biol. 2009; 16:1063–1067. [PubMed: 19749753]
[19]. Coudray N, Valvo S, Hu M, Lasala R, Kim C, Vink M, Zhou M, Provasi D, Filizola M, Tao J, et al. P Natl Acad Sci USA. 2013; 110:2140–2145.
[20]. Das BB, Nothnagel HJ, Lu GJ, Son WS, Tian Y, Marassi FM, Opella SJ. J Am Chem Soc. 2012; 134:2047–2056. [PubMed: 22217388]
[21]. Luo W, Cady SD, Hong M. Biochemistry. 2009; 48:6361–6368. [PubMed: 19489611]
[22]. Park SH, Das BB, Casagrande F, Tian Y, Nothnagel HJ, Chu M, Kiefer H, Maier K, De Angelis AA, Marassi FM, et al. Nature. 2012; 491:779–783. [PubMed: 23086146]
[23]. Haller JD, Schanda P. J Biomol NMR. 2013; 57:263–280. [PubMed: 24105432]
[24]. Andreas LB, Le Marchand T, Jaudzems K, Pintacuda G. J Magn Reson. 2015; 253:36–49. [PubMed: 25797003]
[25]. Barbet-Massin E, Pell AJ, Retel JS, Andreas LB, Jaudzems K, Franks WT, Nieuwkoop AJ, Hiller M, Higman V, Guerry P, et al. J Am Chem Soc. 2014; 136:12489–12497. [PubMed: 25102442]
[26]. Linser R, et al. Angew Chem Int Ed Engl. 2011; 50:4508–4512. [PubMed: 21495136]
[27]. Ward ME, Shi L, Lake E, Krishnamurthy S, Hutchins H, Brown LS, Ladizhansky V. J Am Chem Soc. 2011; 133:17434–17443. [PubMed: 21919530]
[28]. Kurauskas V, Crublet E, Macek P, Kerfah R, Gauto DF, Boisbouvier J, Schanda P. Chem Commun. 2016; 52:9558–9561.
[29]. Hagn F, Etzkorn M, Raschle T, Wagner G. J Am Chem Soc. 2013; 135:1919–1925. [PubMed: 23294159]
[30]. Kijac AZ, Li Y, Sligar SG, Rienstra CM. Biochemistry. 2007; 46:13696–13703. [PubMed: 17985934]
[31]. Renault M, Tommassen-van Boxtel R, Bos MP, Post JA, Tommassen J, Baldus M. P Natl Acad Sci Usa. 2012; 109:4863–4868.
[32]. Jacso T, Franks WT, Rose H, Fink U, Broecker J, Keller S, Oschkinat H, Reif B. Angew Chem Int Ed Engl. 2012; 51:432–435. [PubMed: 22113890]

Europe PMC Funders Author Manuscripts

Europe PMC Funders Author Manuscripts

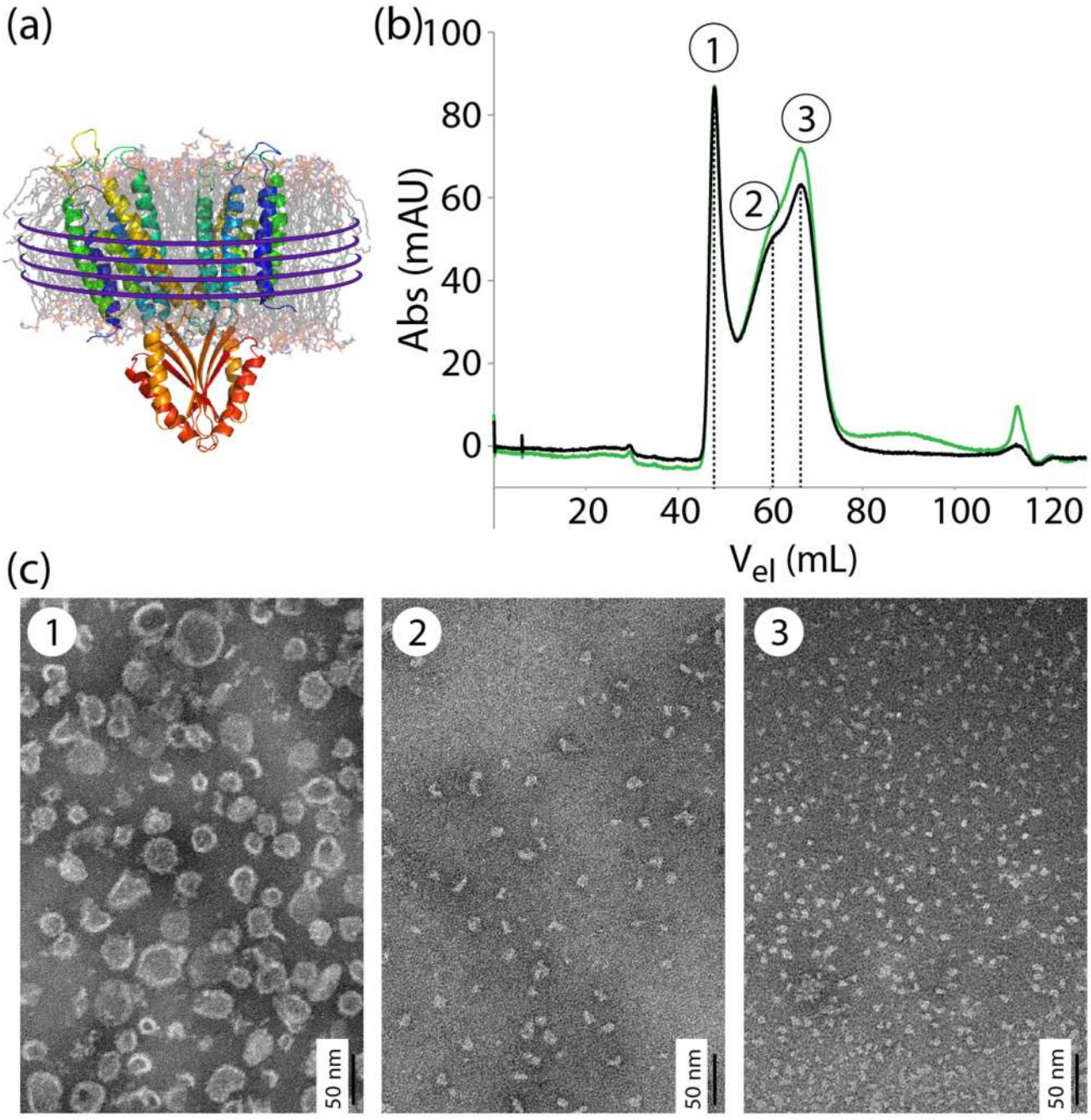


**Figure 1.**

(a) Model of CzcD in a nanodisc, based on a homology model using YiiP.[18] Purple lines schematically denote SMA. (b) Size exclusion chromatogram of SMA_2:1-solubilized CzcD after affinity purification. Elution was followed by measuring the absorption at 280 nm (black) and 260 nm (green). The SMA copolymer shows an absorption maximum around 260 nm. Additional SEC chromatograms are shown in Fig. S3. (c) Negative stain transmission electron micrographs of eluted fractions from (b) collected at the indicated

positions of the chromatogram $V_{el}$ = 47 mL, 58 mL, 68 mL. EM images of a sample after magic-angle spinning are shown in Fig. S5.



Europe PMC Funders Author Manuscripts

Europe PMC Funders Author Manuscripts

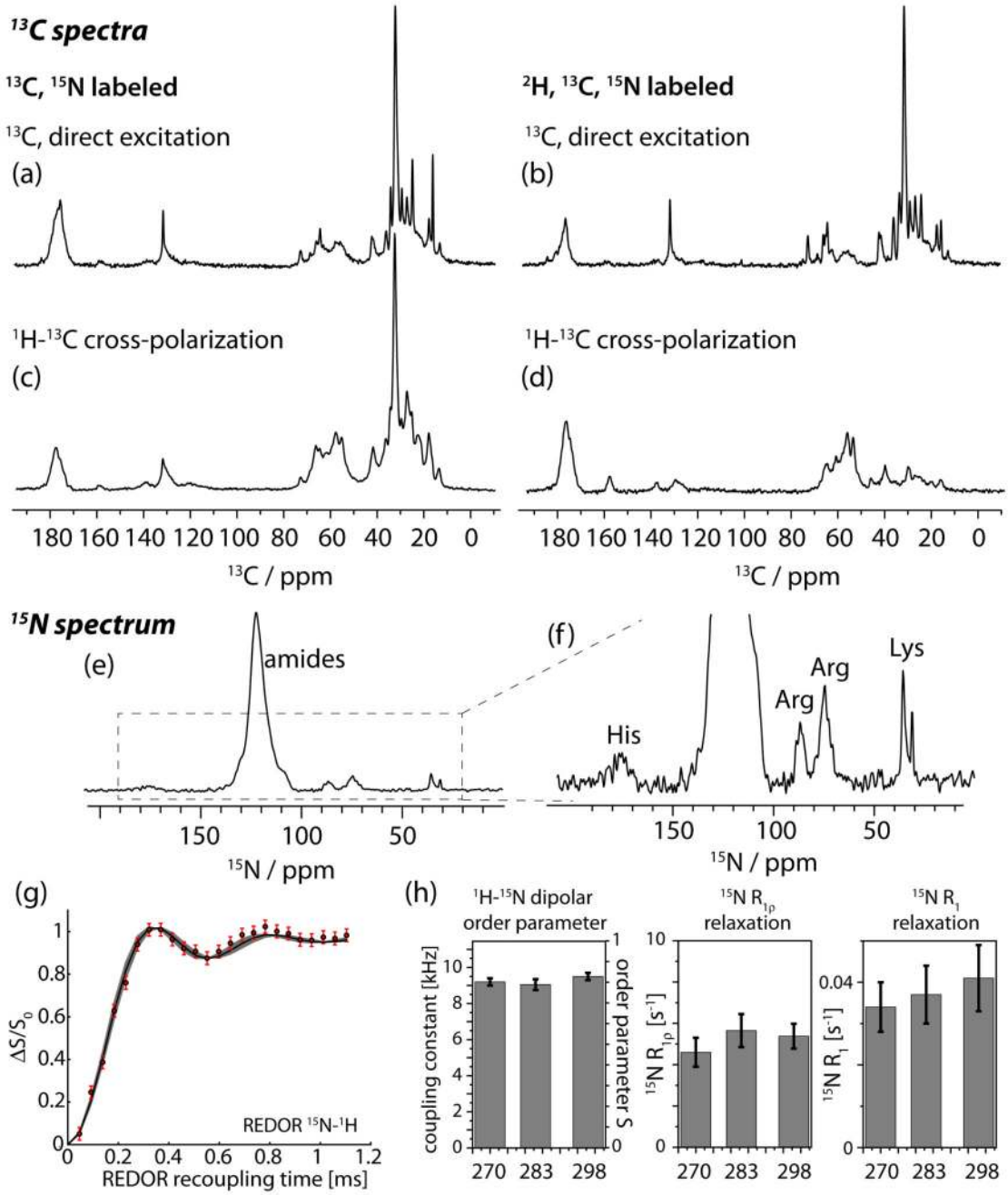


**Figure 2.**

1D NMR characterization of nanodisc-embedded CzcD. $^{13}C$ and $^{15}N$ solid-state NMR spectra of [$^{13}C$,$^{15}N$]- (a,c, e, f) and [$^{2}H$,$^{13}C$,$^{15}N$]-labeled (b, d) CzcD in native nanodiscs, recorded at 55 kHz MAS frequency at 14.1 T static magnetic field strength (600 MHz $^{1}H$ Larmor frequency). (g) REDOR measurement of the bulk $^{1}H$-$^{15}N$ dipolar order parameter. A single fit parameter, the effective coupling constant, is invoked in this fit. (h) Fitted parameters of dipolar couplings, the order parameters derived from the dipolar couplings, and $^{15}N$ relaxation rate constants. Further details are provided in Fig. S8.

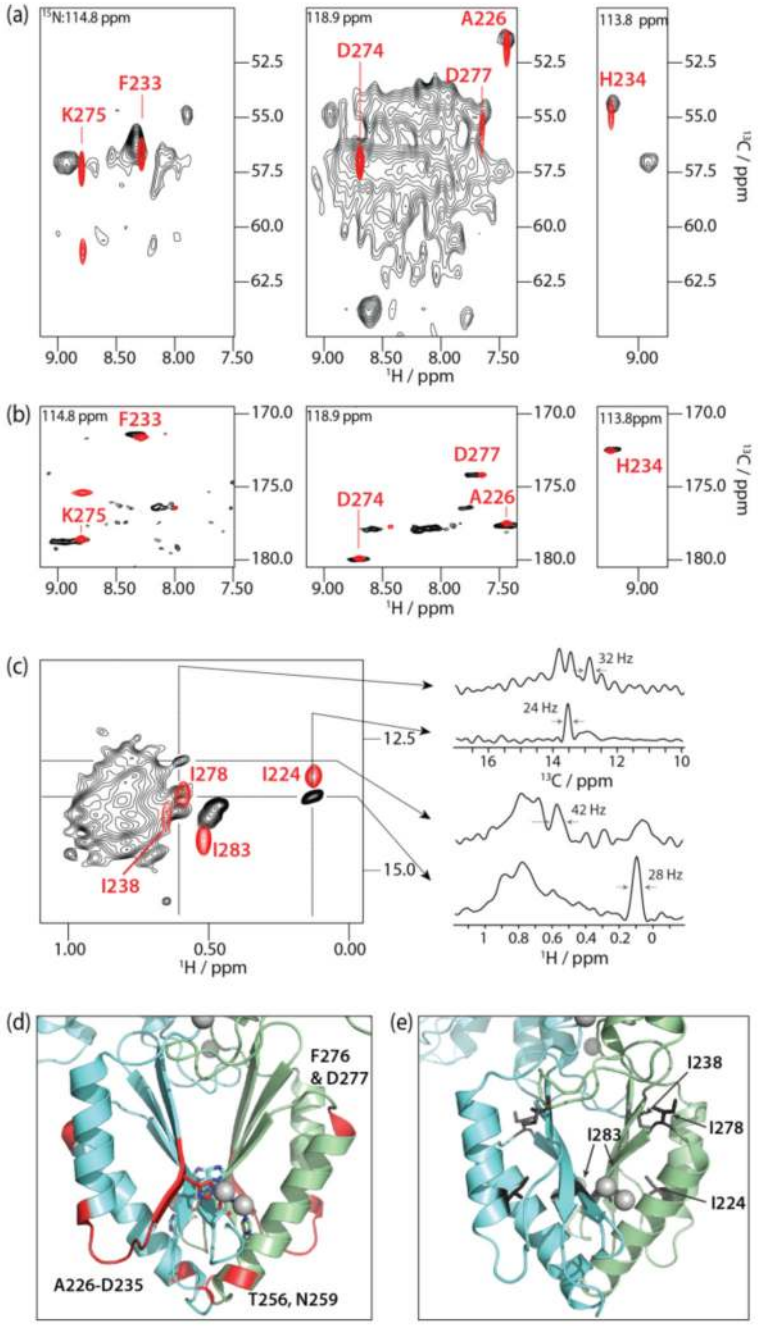


**Figure 3.**

Proton-detected 3D (a,b) and 2D (c) spectra of nanodisc-embedded deuterated CzcD, (a) hCANH and (b) hCONH correlation spectrum of [$^{2}$H,$^{13}$C,$^{15}$N] CzcD obtained at 600 MHz $^{1}$H Larmor frequency and 55 kHz MAS frequency. In addition to the ssNMR spectra, shown in black, solution-state spectra of the soluble domain are overlaid (red). Further views of these spectra are provided in Fig. S9. (c) 2D ssNMR HC spectrum of [$^{2}$H$^{12}$C], Ile-δ1-[$^{13}CH_3$] CzcD (black) and solution-state $^{13}$C-HSQC (red) on [$^{13}$C,$^{15}$N] soluble domain. In all cases, the soluble domain spectra were obtained on a sample containing a two-fold molar

excess of $Zn^{2+}$. (d) Location of the residues identified in the 3D spectra of panels mapped on the YiiP crystal structure (a, b). (e) Localization of the Ile side chains in the cytoplasmic domain within a CzcD homology model.



Europe PMC Funders Author Manuscripts